Therapeutic Targeting Cancer-Initiating Cell Markers by Exosome miRNA: Efficacy and Functional Consequences Exemplified for claudin7 and EpCAM[1]

Daisuke Kyuno[*,2,3], Kun Zhao[*], Nathalie Bauer[*], Eduard Ryschich[†] and Margot Zöller[*,4]

[*]Tumor Cell Biology, University Hospital of Surgery, Heidelberg, Germany; [†]Microcirculation and Cell Migration, University Hospital of Surgery, Heidelberg, Germany

Abstract

AIM: Transfer of exosomes (Exo) miRNA was described interfering with tumor progression. We here explored for claudin7 (cld7) and EpCAM (EpC), cancer-initiating-cell markers in colorectal and pancreatic cancer, the efficacy of Exo loading with miRNA and miRNA transfer. *METHODS:* Exo were collected from nontransformed mouse (NIH3T3) and rat lung fibroblasts (rFb), which were transfected with Tspan8 cDNA (NIH3T3-Tspan8, rFb-Tspan8). Exo were loaded by electroporation with miRNA. The transfer of Exo-miRNA was evaluated *in vitro* and *in vivo* in a rat pancreatic (ASML) and a human colon (SW948) cancer line. *RESULTS:* NIH3T3-Tspan8- or rFb-Tspan8-Exo were efficiently loaded with cld7- or EpC-miRNA. Exo targeting in vivo was strongly improved by tailoring with Tspan8. Exo-miRNA transfer into tumor targets promoted cld7, respectively, EpC downregulation by 33%-60%. Cld7 silencing was accompanied by reduced expression of additional cancer-initiating cell markers and NOTCH. EpC silencing reduced vimentin, N-cadherin, and Nanog expression. The Exo-miRNA transfer affected anchorage-independent growth, motility, and invasion. *CONCLUSIONS:* Exo are efficiently loaded with miRNA, miRNA-delivery being supported by Exo tailoring. Partial cld7 and EpC silencing by Exo miRNA affects metastasis-promoting tumor cell activities. The findings suggest miRNA loading of tailored Exo as an easy approachable and efficient adjuvant therapy.

Translational Oncology (2019) 12, 191–199

Introduction

Metastasis remains the leading cause of cancer death [1]. Tumor progression relies on a small population of cancer-initiating cells (CIC) [2], characterized by sets of function-relevant markers including EpCAM (EpC) and claudin7 (cld7) [3,4].

Claudin7 is a tight junction (TJ) protein [5] that engagement in barrier functions is vital [6,7]. However, cld7 found outside of TJ fulfills distinct functions [5]. Claudin phosphorylation by PKA, PKC, and MLCK prohibits TJ integration and promotes cld internalization [8]. Membrane-integrated palmitoylated cld7 is partitioned into glycolipid-enriched membrane microdomains (GEM) [9,10], with scaffolding functions creating a platform for signal transduction and cytoskeleton reorganization [11]. Palmitoylated cld7 recruits and cooperates with EpC [10,12].

Oncogenic and tumor progression supporting activity of the CIC marker EpC [13] relies on interfering with E-cadherin–mediated adhesion, on its engagement in Wnt/β-catenin signaling, and in

controlling motility by downregulation of PKC and upregulation of MMP7 expression [14]. The cleaved intracellular domain translocates to the nucleus acting as a cotranscription factor for c-myc, cyclin A/E, Oct4, Nanog, and others [15,16].

In view of the contribution of CIC markers to tumor progression, efforts are taken for selective attack. Several studies focused on exosomes (Exo), the most important intercellular communicators [17].

Exo, small vesicles found in all body fluids, consist of a lipid bilayer with integrated membrane proteins. The plasma contains proteins, coding and noncoding RNA and DNA [18]. Exo components are function competent [19]. Exo bind/are taken up by selected targets [20]. Targeting is facilitated by integrin complexes with tetraspanins, in gastrointestinal cancer preferably Tspan8 [21]. Exo uptake severely affects targets [21]. Exo, easy to transfect and storable, could provide powerful therapeutics [22].

Cld7 and EpC contributing to tumor progression, we explored the efficacy of loading Exo from nontransformed cells with cld7- and EpC-specific miRNA. To facilitate Exo uptake, donor cells were transfected with Tspan8. MiRNA transfer, the impact on cld7, EpC and associated molecule expression and metastasis-promoting activities were evaluated.
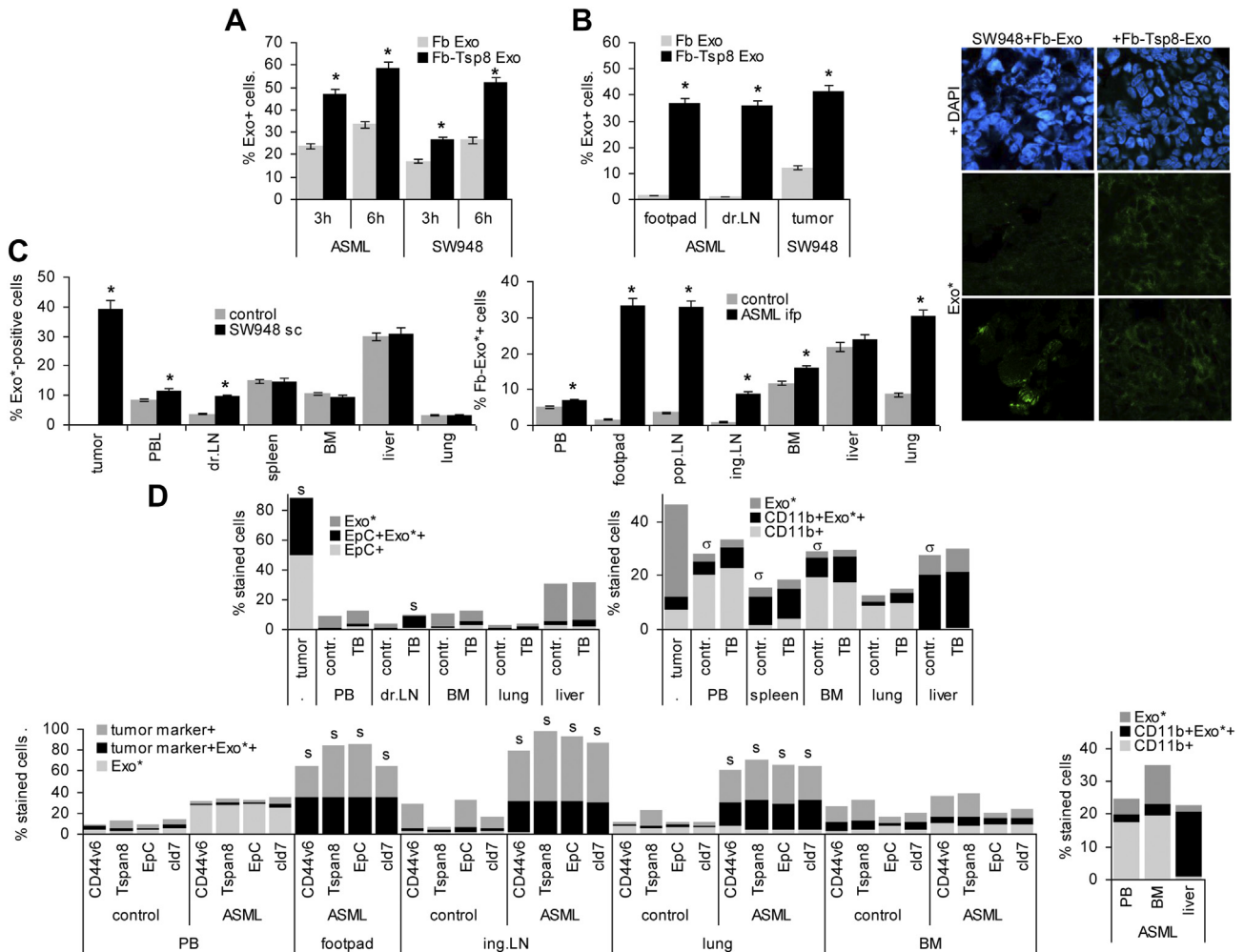
Figure 1. Fibroblast exosome uptake *in vitro* and *in vivo*. (A) Dio-labeled Exo from nontransfected and Tspan8-transfected rFb and NIH3T3 were cocultured for 3 and 6 hours with ASML or SW948 cells. Exo uptake was evaluated by flow cytometry after acid wash to remove bound Exo; mean percent ± SD (triplicates) of stained tumor cells; significant differences between Exo from nontransfected versus transfected Fb: *; (B-D) Dio-labeled Exo and Tspan8-Exo were iv injected into tumor-free and ASML-bearing (ifp application) rats and tumor-free or SW948-bearing (sc injection) nude mice. Animals were sacrificed after 48 hours; organs were excised and meshed. Dio-labeled Exo uptake was evaluated by flow cytometry or confocal microscopy. (B) Flow cytometry analysis of recovery of Dio-labeled Exo and Tspan8-Exo in tumor tissue and confocal microscopy of tumor cells seeded on glass slides (3 examples, 1 counterstained with DAPI (scale bar: 10 μm) are shown). (C) Tumor-free and TB nude mice and rats received a single iv injection of Dio-labeled Tspan8-Exo, flow-cytometry analysis of the percent±SD stained cells (3 animals / group) in the indicated organs; significant differences in Exo uptake between tumor-free and TB animals: *; (D) Tumor-free and TB mice and rats received a single iv injection of Dio-labeled Tspan8-Exo; dispersed cells of the indicated organs were counterstained with the indicated antibodies; the percent of marker+/Exo−, marker+/Exo+ and marker−/Exo + cells (3 animals / group); (B-D) mean (±SD) of triplicates; significant uptake by tumor cells: s, significantly uptake by host cells: σ. Tspan8-overexpressing Exo have an advantage in uptake by tumor cells. High *in vivo* uptake by SW948 tumor tissue and by draining LN and lung of ASML bearing rats relies exclusively on the uptake by tumor cells; comparably high uptake by liver cells and low / medium uptake by SC and BMC largely depends on Mφ and/or MDSC.

Material and Methods

Cell Cultures

Human CoCa SW480, SW948 [23,24], rat PaCa ASML, AS [25], rat lung fibroblasts (rFb) [26], and NIH3T3 were maintained in RPMI1640/10% FCS/glutamine/antibiotics. SW984 and ASML were transiently transfected with miRNA (Primers: TableS1) using HiPerFect according to manufacturer's instructions (Qiagen). Fibroblasts were transfected with Tspan8 cDNA using pcDNA3.1 and standard protocols. NIH3T3-Tspan8 / rFb-Tspan8, selected by single cell cloning, was maintained in RPMI 1640/10% FCS/1.5 µg/ml G418.

Antibodies: see TableS2.

Tissue Preparation

BDX rats and nude mice were sacrificed by cervical dislocation or were anesthetized (CO_2) collecting heparinized peripheral blood (PB) by heart puncture. Organs were excised, shock frozen, or dispersed by meshing through fine gauze.

Exo Collection, Purification, and Transfection

Preparation and SP-Dio$_{18}$(3)-labeling followed described protocols [21], modified by 0.22-µm filtration of cleared supernatants. Exo (20 µg) were transfected with cld7-, EpC-, and transferrin receptor (CD71)-specific miRNA (2 nm miRNA mimics, TableS1) by electroporation [27].

Real-time PCR (qRT-PCR) followed described protocols [26] using GAPDH as internal control for mRNA and small nuclear snRNA U6 for miRNA (primers: Table S1). Statistical analysis was done by the delta-Ct method.

Flow-cytometry of cells and latex bead (LB)-coupled Exo followed standard protocols [26], analyzing samples in a FACSCalibur using the CellQuest program.

Immunoprecipitation (IP), Western Blot (WB)

Lysates (IP: cell-lysate: 500 µg, Exo lysate: 100 µg; WB: cell lysate: 30 µg, Exo lysate: 10 µg) were centrifuged (13,000 g, 10 minutes, 4°C), mixed with antibody (1 hour, 4°C) ,and incubated with Protein G-Sepharose (1 hour). Washed complexes/lysates, dissolved in Laemmli buffer, were resolved on 10%-12% SDS-PAGE. After protein transfer, blocking, and antibody blotting, blots were developed with ECL.

Soft Agar Colonies

Tumor cells in 0.3% agar were seeded on a preformed 1% agar layer. The 0.3% agar contained 30 µg/ml Exo. Colonies were counted after 3 weeks.
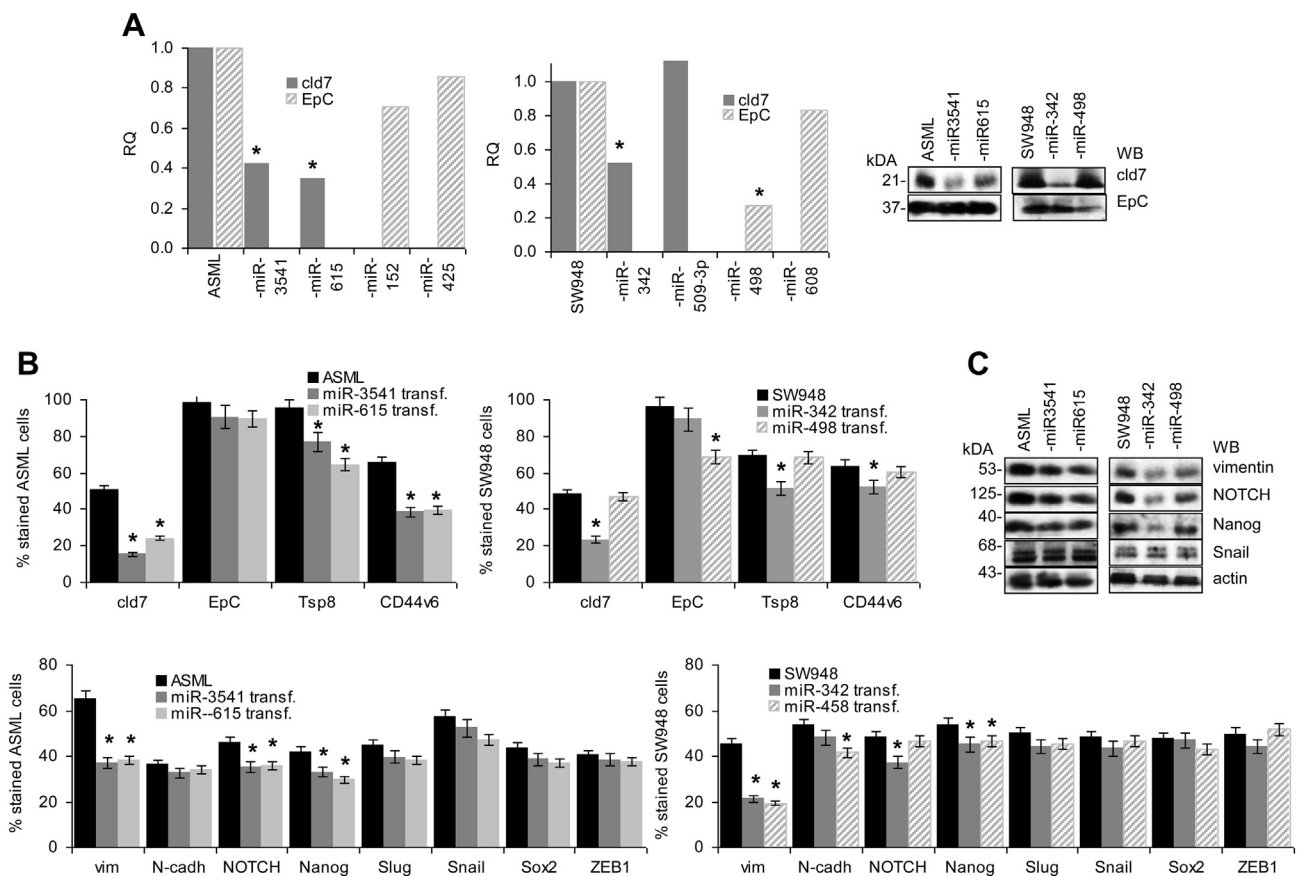
Figure 2. The impact of cld7- and EpC-targeting miRNA on tumor cells. (A) ASML and SW948 cells were transfected with cld7- or EpC-miRNA. After 48 hours, the relative quantity of cld7 and EpC mRNA was evaluated by qRT-PCR and of the proteins by WB. (B) Flow cytometry analysis of CIC markers (cld7, EpC, Tspan8, CD44v6) and EMT markers in miR-3541 and miR-615-transfected ASML and miR-498-and miR-342 transfected SW948 cells; mean percent±SD (triplicates) of stained cells; significant differences between nontransfected and transfected tumor cells: *; (C) representative WB examples of control and miR-transfected ASML and SW948 cells. From eight miRNAs suggested to bind with high confidence to cld7 or EpC mRNA, only two rat cld7-miR and one human cl7- and human-EpC-miR promoted a reduction in cld7, respectively, EpC mRNA and protein expression. Only cld7 downregulation was accompanied by reduced expression of additional CIC markers. Reduced expression of both cld7 and EpC was accompanied by a reduction in vimentin expression. A reduction in the EMT transcription factors Nanog and Notch was restricted to reduced cld7 expression.

In Vitro Wound Healing

A subconfluent monolayer in 24-well plates was scratched with a pipette tip, medium containing 30 µg/ml Exo. Wound closure (light microscopy) was documented as percent wound area at time zero.

Matrigel Invasion

Cells (5 × 104, 200 µl RPMI/1%BSA) were placed on polycarbonate membranes (8 µm pore size) coated with 100 µl 1:5 diluted Matrigel containing 30 µg/ml Exo. The lower chamber contained RPMI/Exo-depleted FCS. After 48 hours, Matrigel invasion and penetration were evaluated microscopically and photometrically after crystal-violet staining.

Exo Uptake In Vitro

Tumor cells were incubated with SP-Dio$_{18}$(3)-labeled Exo. Exo uptake was evaluated by flow cytometry after removal of bound Exo by washing (0.2% HCl/PBS).

Animal Experiments

Exo uptake and distribution were evaluated in nude mice after subcutaneous (sc) injection of 1×10^6 SW948 cells and in BDX rats after intrafootpad (ifp) injection of 1×10^6 ASML cells. When tumors became palpable, tumor-bearing (TB) and control animals received an intravenous (iv) injection of 200 µg SP-Dio$_{18}$(3)-labeled Exo. Animals (3/group) were sacrificed after 48 hours. Animal experiments were Government-approved (Baden-Wuerttemberg, Germany).

Statistics

P values < .05 (in vitro assays: two-tailed Student's t test, in vivo assays: Kruskal-Wallis test) were considered significant.

Results

CIC markers contributing to CIC-Exo-promoted tumor progression [3,28], we explored the feasibility silencing CIC-markers via miRNA-loaded Exo in a human CoCa (SW948) and a rat PaCa (ASML) line, selecting cld7 and EpCAM for monitoring.
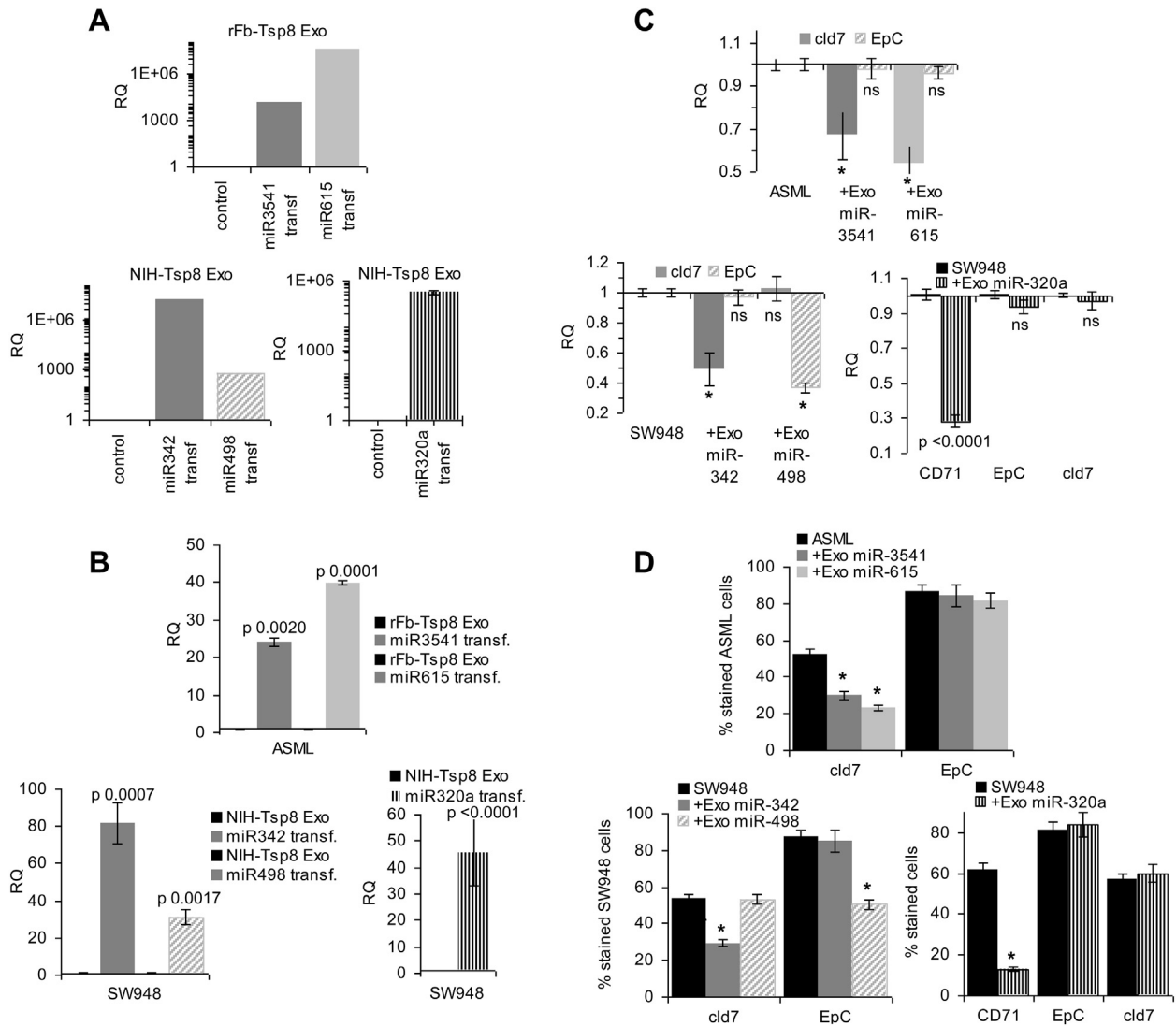
Figure 3. Exosome transfection with miRNA and transfer into tumor cells. (A) Exo were transfected with miRNA by electroporation, and recovery was evaluated by qRT-PCR; mean ± SD (triplicates) are shown; (B-D) SW948 and ASML cells were cocultured for 48 hours with miRNA transfected Fb. (B) Recovery of the miRNA and (C) recovery of cld7, EpCAM, and CD71 mRNA were evaluated by qRT-PCR (mean ± SD of triplicates, significant differences: *) and (D) confirmed for cld7, EpC and CD71 at the protein level by flow cytometry (mean ± SD of triplicates, significant differences by Exo-miR treatment: *). miRNA is efficiently transferred into Exo by electroporation and is recovered in tumor cells after coculture, where it promotes a reduction in cld7, EpC, or CD71, respectively, at the mRNA and the protein level.

Fibroblast Exosomes

NIH3T3 and rFb were used as Exo-donors. Fb were equipped with Tspan8, which facilitates Exo uptake [21].

Flow cytometry and WB of NIH3T3 revealed high CD49f, CD44, and CD106 and low Tspan8 expression. rFb express CD49f, CD104, CD44, N-cadherin (cadh), and VE-cadh at high and Tspan8 at low level, Tspan8 expression being stronger in Exo than cells (Figure S1A, B). NIH3T3 and rFb were transfected with Tspan8 to support Exo-target binding. Expression profiles were not altered with the exception of a slight CD54 upregulation in rFb-Tspan8 and of CD49f and CD106 in NIH3T3-Tspan8 cells and Exo (Fig. S1A,S1B). Tspan8 preferentially associates with α6β4 in rFb- and with α6β1 in NIH3T3-Tspan8 Exo. Tspan8 also associated with CD54 and in Exo with CD44 (rFb) or CD56 and CD106 (NIH3T3 Exo) (Fig. S1C).

To control targeting of Tspan8-Exo, SW948 and ASML were incubated with dio-labeled Exo. Uptake of Tspan8-Exo was increased (>50% of cells) compared to Exo (25%-35% of cells) (Figure 1A). Differences between Exo and Tspan8-Exo were more striking *in vivo*. SW948-bearing (sc) mice and ASML-bearing (ifp) rats were sacrificed 48 hours after 200 μg dio-labeled Exo iv injection. Tumor and the popliteal lymph node (LN) were excised, evaluating recovery of dio-labeled cells in dispersed tissue by flow cytometry. Few cells took up the nontailored Exo, but close to 40% took-up Tspan8-Exo, which was confirmed by confocal microscopy, where NIH3T3-Tspan8 Exo are mostly recovered in tumor cells, whereas NIH3T3 Exo appeared to preferentially bind to the tumor stroma (Figure 1B).

To control for tumor cell uptake, tumor-free and TB animals were sacrificed 48 hours after iv dio-labeled Tspan8-Exo application, evaluating Exo recovery in dispersed tumor tissue, PB, LN, spleen, bone marrow (BM), liver, and lung. In tumor-free animals, Tspan8-Exo were mostly recovered in liver, spleen, BM, and PB. In TB animals, Tspan8-Exo uptake was increased in PB, LN, and in rat BM and lung (Figure 1C). No free Exo were recovered in the serum (not shown). To differentiate between tumor cells and macrophages (Mφ), cells were counterstained. Anti-human EpC staining confirmed Tspan8-Exo uptake in tumor and draining LN. In PB, spleen, BM, and liver of
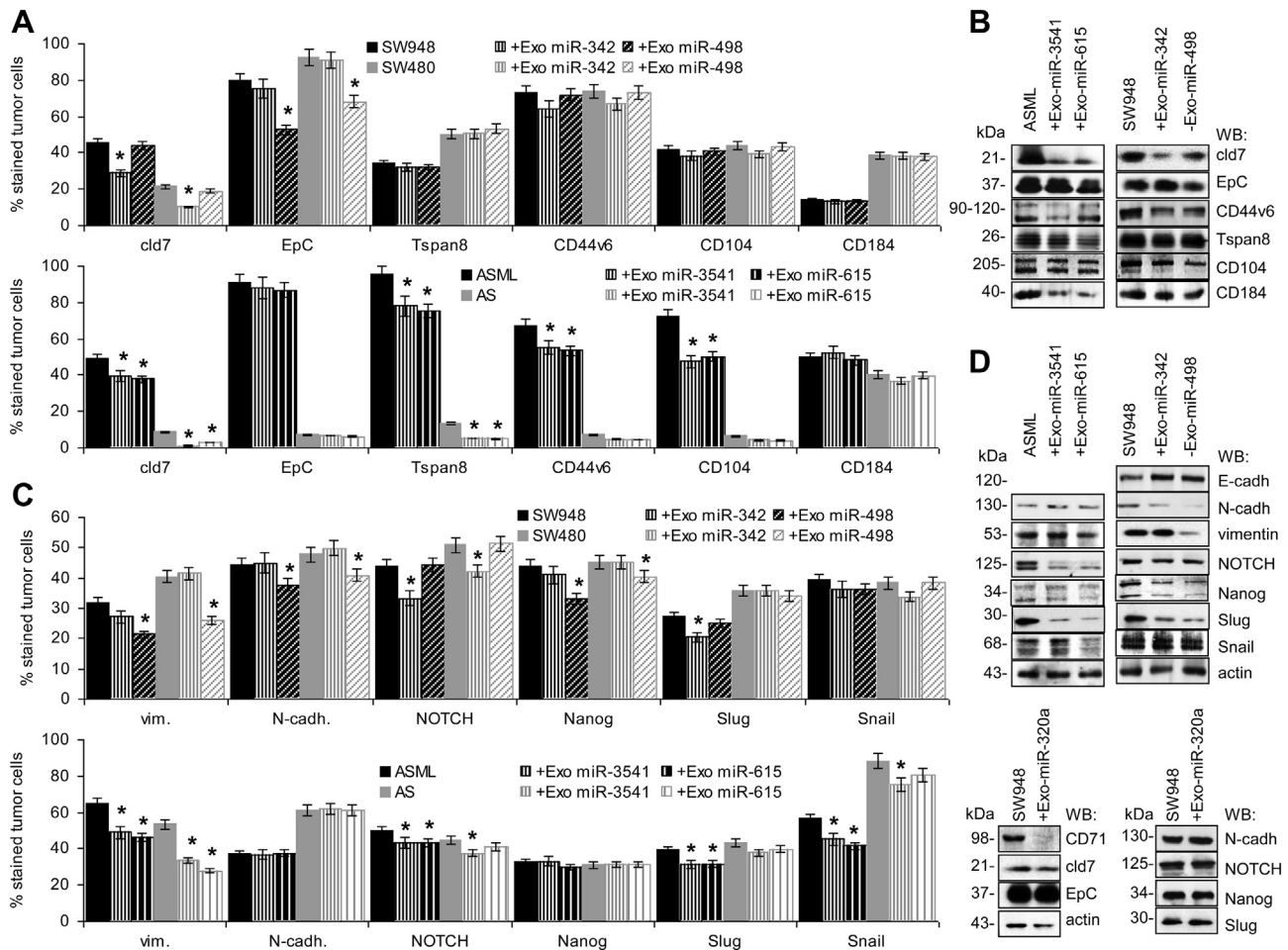
Figure 4. The impact of exosome miRNA transfer into tumor cells on CIC and EMT marker expression. (A-D) miRNA-loaded Exo were cocultured for 48 hours with SW948, SW480, ASML, and AS cells. (A) Flow cytometry analysis of CIC marker and (C) EMT marker expression; mean ± SD of the percent stained cells (three assays); significant differences to cells cocultured with nontransfected Exo: *; (B-D) WB of selected CIC- and EMT-markers after coculture with miR-loaded Exo. The transfer of cld7-miRNA affects expression of additional CIC-markers, particularly CD44v6 and Tspan8. The EMT-markers vimentin N-cadh and E-cadh are more strongly affected by EpC than cld7 silencing. Only cld7 silencing affects NOTCH expression. Nanog expression becomes weakly downregulated by EpC silencing. CD71-miRNA transfer did not affect EMT marker expression.

tumor-free mice Dio + cells were mostly CD11b+. The percent of CD11b+/Dio + cells was slightly increased in PB, BM, and lung of TB mice. Dispersed rat cells were stained with anti-CD44v6, -Tspan8, -EpC, and -cld7. Tspan8-Exo were predominantly taken up by few tumor cells at the injection site, in inguinal LN and lung. CD11b+/ Dio + cells were recovered in BM, PB, and abundantly liver (Figure 1D).
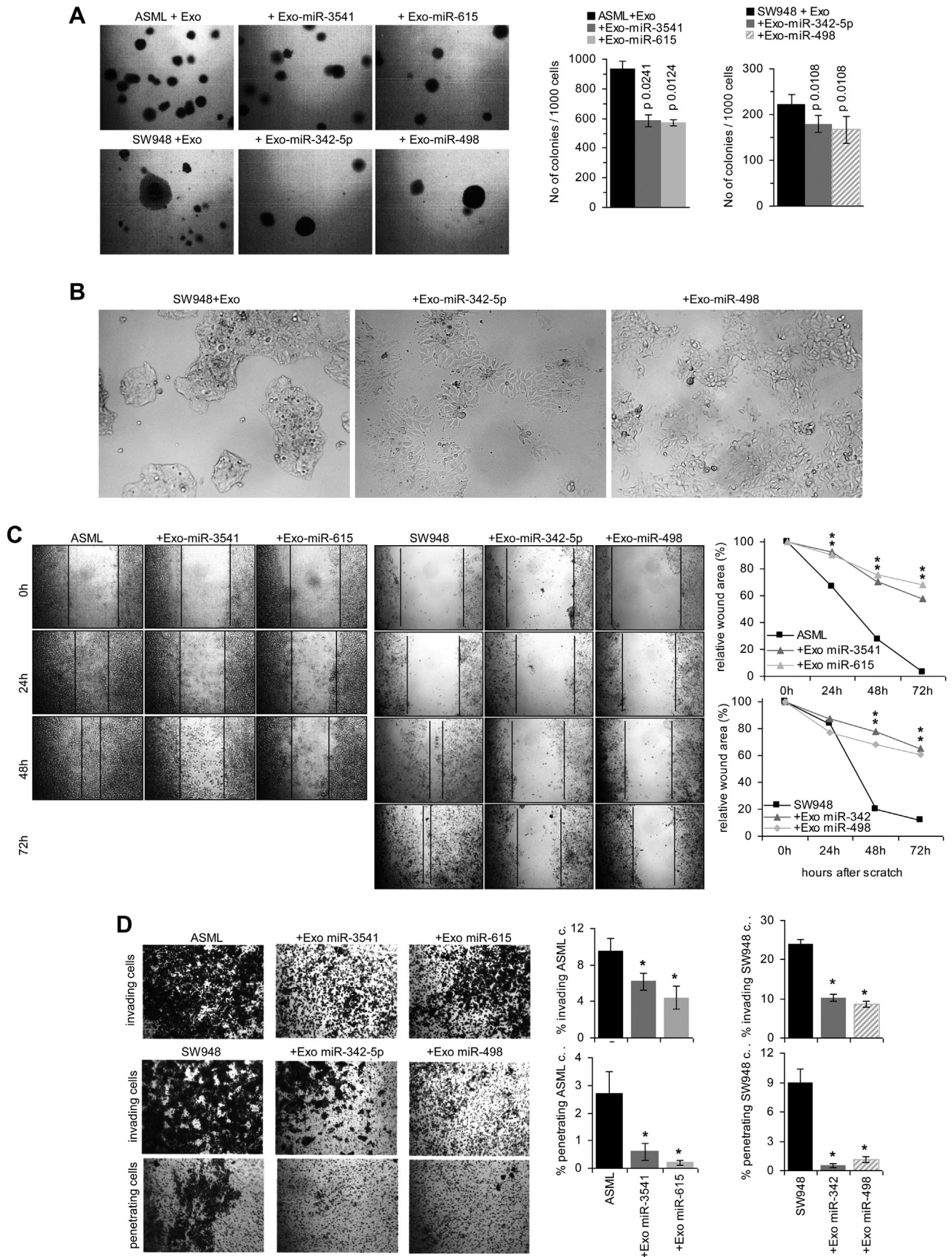
High Tspan8 expression improving Exo uptake by tumor tissue probably relies on Tspan8-associated α6β4 and α6β1 and suffices to deviate from Exo uptake by liver Mϕ. Myeloid-derived suppressor cells may account for slightly increased recovery in PB, BM, and lung of TB animals [29].

Exosome miRNA Loading and miRNA Transfer

The efficacy of miRNA-promoted cld7 and EpC downregulation was first evaluated in tumor cells. MiR-3541 and -615 target rat cld7 and miR-152 and -425 target rat EpC. qRT-PCR 48 hours after ASML transfection revealed a reduction of cld7. Transfection of SW948 cells with cld7-targeting miR-342 reduced cld7 recovery; EpC-targeting miR-609 was inefficient, and miR-498 transfection promoted EpC mRNA reduction. WB confirmed reduced cld7 expression in miR-3541 and miR-615 transfected ASML. In SW948, miR-342 transfection reduced cld7, and miR-498 reduced EpC expression (Figure 2A). Cld7-specific miRNA additionally affected CD44v6 and Tspan8 expression. Transfection with EpC- and cld7-specific miRNA was accompanied by slightly reduced vimentin and Nanog expression. A slight reduction of NOTCH was seen after cld7 mRNA downregulation and of N-cadh after EpC mRNA downregulation, which was confirmed by WB (Figure 2B,C).

qRT-PCR after miRNA-transfection of Tspan8-Exo showed RQ values between $>6 \times 10^3$ to $>3 \times 10^6$. This also accounted for miR-320a that targets CD71 and was included as control (Figure 3A). RQ values after culturing tumor cells for 48 h with miRNA transfected Tspan8-Exo were in the range of 24- to 82 fold compared to coculture with unloaded Exo (Figure 3B). After coculture with miRNA-loaded Exo, cld7 mRNA was reduced by 33%-51% in ASML; EpC was reduced by 60%, cld7 by 55%, and CD71 by 72% in SW948 cells (Figure 3C). A comparable reduction was seen at the protein level (flow-cytometry), which confirmed the selectivity of the miRNA-loaded Exo coculture, where miR-3541 and miR-615 reduced cld7 in ASML cells by 50% to 60%. MiR-342 reduced cld7 expression by >50%, miR-498 reduced EpC expression by >40%, and miR-340a promoted a reduction of CD71 expression by 90%. In all instances, reduced protein expression was restricted to the miRNA specificity (Figure 3C, Figure S2A).

Tspan8-Exo are efficiently loaded with miRNA, and Exo miRNA is transferred into tumor cells. Transferred miRNA selectively affected the respective mRNA/protein expression. However, transfer efficacy remaining below that upon direct miRNA transfection, the question arose on impaired metastasis-promoting activities.

Target Modulation by Exosome miRNA Transfer

A cld7kd and an EpCkd indicated engagement in EMT marker and EMT-related transcription factor expression, a loss in anchorage-independent growth, reduced migration and invasion [10,30]. These cld7- and EpC-promoted activities were chosen controlling for the efficacy of transferred miRNA.

CIC marker and EMT gene expression was evaluated in SW948, SW480 (CoCa), ASML and AS, a nonmetastasizing ASML subline [25], SW480 and AS cells showing low cld7 expression. Flow cytometry and WB revealed cld7 and EpC downregulation in SW948 and SW480 cells cultured with miRNA-loaded Tspan8-Exo. Cld7-miR transfected rFb-Tspan8-Exo promoted cld7 and slightly reduced Tspan8, CD44v6, and CD104 expression (Figure 4A, Figure S2B, Figure 4B). The EMT markers vimentin and N-cadh became more strongly downregulated by EpC- than cld7-miRNA-loaded Exo. NOTCH and Slug expression was slightly reduced after coculture with cld7-miR-transfected Exo. EpC-miR weakly affected Nanog expression (Figure 4C, Figure S2C). WB confirmed the stronger impact of EpC-miRNA on vimentin, N-cadh, E-cadh, and Nanog. Instead, coculture with miR-320a–loaded NIH-Tspan8-Exo, though promoting CD71 downregulation, did not affect N-cadh, NOTCH, Nanog, and Slug expression (Figure 4D).

Fb-Exo miRNA transfer affecting CIC and EMT marker protein expression alike a cld7kd or EpCkd, though with lower efficacy, functional consequences were evaluated.

Coculture with cld7- and EpC-miRNA-loaded Exo sufficed for reduced anchorage-independent growth, the number of soft agar colonies developing in the presence of unloaded and EpC-miR or cld7-miR-loaded Exo differing significantly (Figure 5A).

Furthermore, in SW948 cells cultured with cld7-miR–loaded Exo, a loss of tightly packed cell clusters was seen such that individual cell boundaries became clearly visible, possibly indicating a loss of TJ. After coculture with EpC-miR–loaded Exo, cells displayed a rounder shape (Figure 5B).

In vitro wound healing after scratching a subconfluent monolayer was strongly impaired in the presence of miR-transfected Exo (Figure 5C). The transfer of cld7- and EpC-miRNA-loaded Exo also affected invasiveness. Cells were cocultured with miR-loaded Exo for 48 hours and thereafter seeded on Exo-miR containing Matrigel. The lower well contained medium with Exo-depleted FCS. Matrigel invasion was significantly reduced, and penetration was nearly abolished in SW948 and poorly Matrigel-penetrating ASML cells (Figure 5D).

Impaired anchorage-independent growth, migration, and invasion confirmed transferred cld7- and EpC-specific miRNA affecting CIC activities.

Discussion

Fb-Exo transfection with miRNA is highly efficient. Tailoring Exo facilitates Exo uptake, transferred Exo miRNA being function-competent.

Figure 5. The impact of exosome miRNA transferred into tumor cells on tumor progression-associated activities. (A-F) ASML and SW948 cells were cocultured for 48 hours with 30 μg/ml miRNA transfected Exo, where indicated Exo also were included during the assay period. (A) Exo-treated tumor cells were seeded in 0.3% agar containing 30 μg/ml Exo on a 1% agar monolayer. Cells were cultured for 3 weeks. Thereafter, the number of soft agar colonies was counted; representative examples and mean $\pm$ SD of 10 wells are shown; significant differences between cocultures with nontransfected versus transfected Exo are indicated; (B) Morphology of SW948 cells after 48-hour culture in the presence of nontransfected and miRNA-transfected Exo; (C) SW948 and ASML cells were seeded in 24-well plates and cultured in the presence of unloaded or miR-loaded Exo. Reaching subconfluence, medium was exchanged, and the monolayer was scratched with a yellow pipette tip. Wound healing was followed for 72 hours by light microscopy. Representative examples and the mean (five wells) of the wound area as % of the starting wound area are shown; significant differences between treatment with unloaded and miRNA-loaded Exo: *; (D) Exo-treated ASML and SW948 cells were seeded on Matrigel in 48-Transwell plates; the Matrigel contained 30 μg/ml Exo, and the lower chamber contained medium with Exo-depleted FCS. After 48 hours, invading cells (OD595 after lysis and crystal violet staining) and penetrating cells (counting after crystal violet staining) were evaluated. Representative examples and mean $\pm$ SD (five wells) as % of the seeded number of cells are shown; significant differences between treatment with unloaded versus miRNA-loaded Exo: *.The transfer of cld7- or EpC-miRNA affects anchorage-independent growth, migration, and invasion.

Tailoring Exosomes

Exo uptake mostly occurs via receptor binding and internalization [31]. Monocytes, particularly liver-resident Mφ [32], are most prevalent targets in the absence of more avidly binding structures. In the presence of appropriate targets, Exo become redirected, well explored for dendritic cell Exo binding to immunological synapses [33] and tumor Exo binding in metastasis-prone organs and to endothelial cells [34,35]. The "selectivity" of Exo binding depends on clustered molecules, e.g., tetraspanin complexes, allowing for multiple binding [21,36], Tspan8 being the preferred partner in gastrointestinal cancer [4,37,38]. Based on this information, Fb abundantly expressing α6 were Tspan8 transfected, which sufficed for uptake redirection.

For therapeutic application, tailoring Exo towards the strived target is important. Tetraspanin complexes provide such a targeting unit. Controlling for tetraspanin-associated molecule expression avoids the requirement of double transfection.

Exosome miRNA Transfection and miRNA Transfer

From several miRNA with a high score for rat, respectively, human cld7 and EpC, only two rat cld7-specific miRNA and one human cld7- and one EpC-specific miRNA sufficed for a significant reduction in the tumor cells and were used for Exo electroporation, a transferrin receptor-specific miRNA serving as control.

Culturing tumor cells with miRNA-loaded Exo provoked a significant but selective cld7, respectively, EpC or CD71 mRNA and protein decrease, which was confirmed in additional lines. Only in ASML cells was a concomitant slight Tspan8, CD104, and CD44v6 reduction by cld7 silencing seen. This might be due to the majority of cld7, Tspan8, CD44v6, and CD104 being clustered in GEM in ASML cells [37,38]. EpC-miRNA transfer was accompanied by slightly reduced vimentin and N-cadh and increased E-cadh expression. NOTCH and Snail expression was slightly decreased after culture with cld7-miR-Exo. EpC-miR-Exo affected Nanog and Slug expression. CD71 miR-loaded Exo exerted none of these effects. Differences between ASML and SW948 cells might rely on the absence of TJ and E-cadh expression and the particularly strong cld7 and EpC recruitment into GEM in ASML cells [10], versus the dominating integration of cld7 in TJ and the abundance of free EpC in CoCa lines [9].

Briefly, Fb-Exo are efficiently loaded with miRNA and miRNA-loaded Exo silence selectively cld7, EpC, and CD71 expression in targets. The transfer of Exo cld7- and EpC-miR can affect additional CIC markers (ASML), EMT markers (preferentially EpC-miRNA), and EMT-related transcription factors. As these effects were weak and varied between targets, a higher Exo dose (30 μg/ml) was used in functional assays.

MiRNA, Anchorage-Independent Growth, Motility, and Invasion

Cld7- and EpC-specific Exo miRNA impaired anchorage-independent growth with comparable efficacy. A Tsp8kd, CD44v6kd, cld7kd, or EpCkd each sufficing for strongly impaired anchorage-independent growth [10,30,38], suggests this CIC feature requiring the complex of the four molecules. The efficacy of an Exo cld7- and EpC-miRNA transfer strengthens the interpretation.

Like cld7kd and EpCkd cells [10,30], motility and invasion become mitigated by the cld7- and EpC-miRNA transfer. Reduced migration fits with cld7 / EpC-cld7 associating with cytoskeletal linker proteins [12,30] promoting actin reorganization [39]. The association with integrins in GEM may sustain motility by integrin

and downstream signaling activation [40]. The missing MMP regulation in cld7ko mice and MMP9 downregulation in cld7kd tumors [6,10] match reduced invasiveness by cld7- and EpC-miR.

The cld7- and EpC-miRNA transfer from Exo into tumor cells recapitulating the impact of a ko / kd is promising for silencing metastasis-promoting genes by miRNA-loaded Exo.

Conclusion

Attacking CIC markers via miRNA-loaded Exo is a promising option fighting metastasis.

Exo being efficiently loaded with miRNA, four points need consideration. 1) Exo of nontransformed cells eliminates the risk of oncogenic transformation. Easy to grow fibroblasts are suitable Exo donors. 2) Frequently being expressed by a restricted cell number and/or at low density, reducing the risk impairing physiological functions, CIC markers could be a prime miRNA target. 3) Equipping Exo with binding units is essential. We built on previous work demonstrating Exo Tspan8-α6β4 complexes assisting uptake by PaCa and CoCa. However, Exo tailoring needs exploration for the envisaged targets, which accounts for the adhesion molecule and the associating tetraspanin. 4) The impact on metastasis-promoting activities requires amendment achieved by loading Exo with a panel of miRNA or, should the uptake capacity provide an undue limit, transfecting aliquots of Exo with distinct miRNA. These requirements being technically easy to handle, Exo loaded with CIC-marker-specific miRNA could become a promising adjuvant cancer therapy [3,17].

Authors' Contribution

D. K., K. Z., N. T., and M. Z. performed and analyzed experiments; M. Z. planned and analyzed experiments and wrote the manuscript, corrected by E.R. and approved by all authors.

Conflict of Interest

All authors declare no conflict of interest.

Appendix A. Supplementary data

Supplementary data to this article can be found online at https://doi.org/10.1016/j.tranon.2018.08.021.

References

[1] Siegel RL, Miller KD, and Jemal A (2016). Cancer statistics, 2016. *CA Cancer J Clin* **66**, 7–30.

[2] Elshamy WM and Duhé RJ (2013). Overview: cellular plasticity, cancer stem cells and metastasis. *Cancer Lett* **341**, 2–8.

[3] Murar M and Vaidya A (2015). Cancer stem cell markers: premises and prospects. *Biomark Med* **9**, 1331–1342.

[4] Wang H, Rana S, Giese N, Büchler MW, and Zöller M (2013). Tspan8, CD44v6 and alpha6beta4 are biomarkers of migrating pancreatic cancer-initiating cells. *Int J Cancer* **133**, 416–426.

[5] Van Itallie CM and Anderson JM (2014). Architecture of tight junctions and principles of molecular composition. *Semin Cell Dev Biol* **36**, 157–165.

[6] Ding L, Lu Z, Foreman O, Tatum R, Lu Q, and Renegar R, et al (2012). Inflammation and disruption of the mucosal architecture in claudin-7-deficient mice. *Gastroenterology* **142**, 305–315.

[7] Tanaka H, Takechi M, Kiyonari H, Shioi G, Tamura A, and Tsukita S (2015). Intestinal deletion of Claudin-7 enhances paracellular organic solute flux and initiates colonic inflammation in mice. *Gut* **64**, 1529–1538.

[8] Su L, Nalle SC, Shen L, Turner ES, Singh G, and Breskin LA, et al (2013). TNFR2 activates MLCK-dependent tight junction dysregulation to cause apoptosis-mediated barrier loss and experimental colitis. *Gastroenterology* **145**, 407–415.

[9] Tauro BJ, Greening DW, Mathias RA, Mathivanan S, Ji H, and Simpson RJ (2013). Two distinct populations of exosomes are released from LIM1863 colon carcinoma cell-derived organoids. *Mol Cell Proteomics* **12**, 587–598.

[10] Thuma F, Heiler S, Schnölzer M, and Zöller M (2016). Palmitoylated claudin7 captured in glycolipid-enriched membrane microdomains promotes metastasis via associated transmembrane and cytosolic molecules. *Oncotarget* **7**, 30659–30677.

[11] Mollinedo F and Gajate C (2015). Lipid rafts as major platforms for signaling regulation in cancer. *Adv Biol Regul* **57**, 130–146.

[12] Heiler S, Mu W, Zöller M, and Thuma F (2015). The importance of claudin-7 palmitoylation on membrane subdomain localization and metastasis-promoting activities. *Cell Commun Signal* **13**, 29.

[13] Imrich S, Hachmeister M, and Gires O (2012). EpCAM and its potential role in tumor-initiating cells. *Cell Adh Migr* **6**, 30–38.

[14] Maghzal N, Vogt E, Reintsch W, Fraser JS, and Fagotto F (2010). The tumor-associated EpCAM regulates morphogenetic movements through intracellular signaling. *J Cell Biol* **191**, 645–659.

[15] Maetzel D, Denzel S, Mack B, Eggert C, Bärr G, and Gires O (2009). Nuclear signalling by tumour-associated antigen EpCAM. *Nat Cell Biol* **11**, 162–171.

[16] Lin CW, Liao MY, Lin WW, Wang YP, Lu TY, and Wu HC (2012). Epithelial cell adhesion molecule regulates tumor initiation and tumorigenesis via activating reprogramming factors and epithelial-mesenchymal transition genes expression in colon cancer. *J Biol Chem* **287**, 39449–39459.

[17] Wang J, Zheng Y, and Zhao M (2017). Exosome-based cancer therapy: implication for targeting cancer stem cells. *Front Pharmacol* **7**, 533.

[18] Kalra H, Drummen GP, and Mathivanan S (2016). Focus on extracellular vesicles: introducing the next small big thing. *Int J Mol Sci* **17**, 170.

[19] Lo Cicero A, Stahl PD, and Raposo G (2015). Extracellular vesicles shuffling intercellular messages: for good or for bad. *Curr Opin Cell Biol* **35**, 69–77.

[20] French KC, Antonyak MA, and Cerione RA (2017). Extracellular vesicle docking at the cellular port: Extracellular vesicle binding and uptake. *Semin Cell Dev Biol* **67**, 48–55.

[21] Rana S, Yue S, Stadel D, and Zöller M (2012). Toward tailored exosomes: the exosomal tetraspanin web contributes to target cell selection. *Int J Biochem Cell Biol* **44**, 1574–1584.

[22] Conlan RS, Pisano S, Oliveira MI, Ferrari M, and Mendes Pinto I (2017). Exosomes as reconfigurable therapeutic systems. *Trends Mol Med* **23**, 636–650.

[23] Trainer DL, Kline T, McCabe FL, Faucette LF, Feild J, and Chaikin M, et al (1988). Biological characterization and oncogene expression inhuman colorectal carcinoma cell lines. *Int J Cancer* **41**, 287–296.

[24] Leibovitz A, Stinson JC, McCombs III WB, McCoy CE, Mazur KC, and Mabry ND (1976). Classification of human colorectaladenocarcinoma cell lines. *Cancer Res* **36**, 4562–4569.

[25] Matzku S, Komitowski D, Mildenberger M, and Zöller M (1983). Characterization of BSp73, a spontaneous rat tumor and its in vivo selected variants showing different metastasizing capacities. *Invasion Metastasis* **3**, 109–123.

[26] Rana S, Malinowska K, and Zöller M (2013). Exosomal tumor microRNA modulates premetastatic organ cells. *Neoplasia* **15**, 281–295.

[27] Zhang D, Lee H, Zhu Z, Minhas JK, and Jin Y (2017). Enrichment of selective miRNAs in exosomes and delivery of exosomal miRNAs in vitro and in vivo. *Am J Physiol Lung Cell Mol Physiol* **312**, L110–L121.

[28] Desrochers LM, Antonyak MA, and Cerione RA (2016). Extracellular vesicles: satellites of information transfer in cancer and stem cell biology. *Dev Cell* **37**, 301–309.

[29] Zöller M (2018). Janus-faced myeloid-derived suppressor cell exosomes for the good and the bad in cancer and autoimmune disease. *Front Immunol* **9**, 137.

[30] Philip R, Heiler S, Mu W, Büchler MW, Zöller M, and Thuma F (2015). Claudin-7 promotes the epithelial-mesenchymal transition in human colorectal cancer. *Oncotarget* **6**, 2046–2063.

[31] Mulcahy LA, Pink RC, and Carter DR (2014). Routes and mechanisms of extracellular vesicle uptake. *J Extracell Vesicles* **3**.

[32] Koh E, Lee EJ, Nam GH, Hong Y, Cho E, and Yang Y, et al (2017). Exosome-SIRPα, a CD47 blockade increases cancer cell phagocytosis. *Biomaterials* **121**, 121–129.

[33] Mittelbrunn M, Vicente Manzanares M, and Sánchez-Madrid F (2015). Organizing polarized delivery of exosomes at synapses. *Traffic* **16**, 327–337.

[34] Grange C, Tapparo M, Collino F, Vitillo L, Damasco C, and Deregibus MC, et al (2011). Microvesicles released from human renal cancer stem cells stimulate angiogenesis and formation of lung premetastatic niche. *Cancer Res* **71**, 5346–5356.

[35] Hoshino A, Costa-Silva B, Shen TL, Rodrigues G, Hashimoto A, and Tesic Mark M, et al (2015). Tumour exosome integrins determine organotropic metastasis. *Nature* **527**, 329–335.

[36] McKelvey KJ, Powell KL, Ashton AW, Morris JM, and McCracken SA (2015). Exosomes: mechanisms of uptake. *J Circ Biomark* **4**, 7.

[37] Yue S, Mu W, Erb U, and Zöller M (2015). The tetraspanins CD151 and Tspan8 are essential exosome components for the crosstalk between cancer initiating cells and their surrounding. *Oncotarget* **6**, 2366–2384.

[38] Wang Z, von Au A, Schnölzer M, Hackert T, and Zöller M (2016). CD44v6-competent tumor exosomes promote motility, invasion and cancer-initiating cell marker expression in pancreatic and colorectal cancer cells. *Oncotarget* **7**, 55409–55436.

[39] Haynes J, Srivastava J, Madson N, Wittmann T, and Barber DL (2011). Dynamic actin remodeling during epithelial-mesenchymal transition depends on increased moesin expression. *Mol Biol Cell* **22**, 4750–4764.

[40] Termini CM and Gillette JM (2017). Tetraspanins function as regulators of cellular signaling. *Front Cell Dev Biol* **5**, 34.